AEGC Australasian Exploration Geoscience Conference Brisbane 2021

Examples of integrating hyperspectral, geochemical and petrophysical drill core data using Australia's National Virtual Core Library infrastructure

Carsten Laukamp[1)], Jessica Stromberg, Neil Francis, Shane Mulè, Monica LeGras, Juerg Hauser, Ian C. Lau
CSIRO Mineral Resources
26 Dick Perry Avenue, Kensington 6151 WA, Australia
[1)]Carsten.Laukamp@csiro.au

SUMMARY

Drill core analytical tools are used for objectively measuring geoscience parameters that aid mineral exploration or groundwater research. Multiple types of geoscience parameters are frequently compared alongside each other, but underlying physicochemical relationships are seldom explored. If the relationships between different parameters are understood, 1) expensive measurements can be inferred from more cost-effective measurements and 2) workflows can be developed that enable fast and objective selection of samples for further, more time-consuming sample analysis. Ultimately, linking geophysical, geochemical and mineralogical parameters could give rise to a new generation of higher-level geoscience products reconciling different sources of information. This paper describes some of the causative relationships between hyperspectral, geochemical and petrophysical data using drill core data sets made available by AuScope's National Virtual Core Library (NVCL) infrastructure program.

Key words: reflectance spectra, mineral chemistry, gamma logs, density, magnetic susceptibility.

INTRODUCTION

The aim of this abstract is to summarise some of the causative relationships between hyperspectral, geochemical and petrophysical data and using drill core data sets available through AuScope's NVCL infrastructure program. Reflectance spectra in this abstract are categorised in the following wavelength regions: Visible-near infrared (VNIR; 380 nm to 1200 nm), shortwave infrared (SWIR; 1200 nm to 2500 nm), mid infrared (MIR; 2500 nm to 5500 nm), and thermal infrared (TIR; 5500 nm to 15,000 nm).

Causative relation between geochemical and hyperspectral data

Hyperspectral reflectance spectra contain information about molecules and elements present in the measured sample. Ultraviolet, visible and infrared light is absorbed at frequencies specific to the respective functional group or chemical element, generating characteristic patterns of absorption bands that are the fingerprints of minerals (Burns, 1993; Clark et al., 1990; Laukamp et al., 2021c).

A direct link between hyperspectral and geochemical data, for example, using a HyLogger3 (Schodlok et al., 2016) and X-ray fluorescence (XRF) respectively, can be drawn in many cases. For example, potassium in felsic igneous rocks is predominantly contained within micas and K-feldspars. Hyperspectral data collected in wavelength regions where these mineral groups are active (i.e. white mica: 2190 to 2450 nm and 8000 to 10,000 nm, or K-feldspar: 8000 to 10,000 nm) often show a strong correlation with potassium derived from whole-rock geochemistry. An example is shown in Figure 1, which features whole rock geochemistry and hyperspectral reflectance spectra collected from tray 46 of drill core C3DD024 (Greenbushes, Western Australia). The potassium content normalised by silica content (i.e. K_2O/SiO_2) shows significant variation in the four intervals of drill core tray 46. Changes in K_2O/SiO_2 correspond with the most prominent TIR-active mineral species as identified by means of the mineral unmixing algorithm jCLST built into The Spectral Geologist Software package TSG™ (https://research.csiro.au/thespectralgeologist/), with increased abundance of K-feldspar in intervals with elevated K_2O/SiO_2. (i.e. 168.3 to 169.2 m and 170.1 to 171.2 m depth). However, a detailed comparison of TIR reflectance spectra collected at 1 cm steps with whole rock geochemistry, reveals that the amount of K-feldspar relative to other minerals varies significantly within the 1 m interval analysed for whole rock geochemistry.

The hyperspectral resolution of drill core and field spectrometers allows the extraction of geochemical exchange vectors at a quality comparable to electron microprobe measurements. Exchange vectors commonly inferred from hyperspectral data include the Tschermaks exchange in white micas (Vedder and McDonald, 1963) and the Mg/(Mg+Fe) ratio in chlorites (McLeod et al., 1987). Beyond these, there are numerous more exchange vectors that can potentially be extracted from hyperspectral reflectance spectra, such as from the fundamental OH vibrations in the MIR. A summary of exchange vectors commonly tracked in mineral exploration is provided in (Laukamp et al., 2021a).

The estimation of the abundance of certain minerals from wavelength ranges where these mineral groups are not active is problematic, relying on co-occurrence in mineral assemblages. An example is the estimation of garnet and pyroxene abundance from VNIR reflectance spectra. Both mineral groups may show features in the VNIR wavelength range resulting from their respective transition element composition. However, while these features may be indicative of, for example, iron-rich garnet and pyroxene (e.g. aegirine, almandine, hedenbergite), they neither reliably identify their presence nor correspond with their abundance. Instead, garnet and pyroxene abundance can be estimated from the TIR wavelength range where both mineral groups produce diagnostic features (Laukamp et al., 2021b).

Causative relation between petrophysical and hyperspectral data

In a mineral exploration context, petrophysical borehole information is commonly used to verify the results of geophysical inversion. Enhancing geophysical inversions through borehole information relies on the development of tools that are at the intersection between borehole focused datasets (e.g. hyperspectral, electrical resistivity logs) and geophysical datasets (e.g. airborne electromagnetic surveys). For this, the causal relationships between mineralogical and petrophysical data must be understood and inversion algorithms need to be formulated that allow to account for this type of complex prior information.

Table 1 lists some of the mineral groups or mineral species with different petrophysical properties, as well as the wavelength ranges they show absorption features in and other rock properties that impact on both, the respective petrophysical measurements and the reflectance spectra. Previous published comparisons of hyperspectral drill core and petrophysical data are sparse. A comparison of total gamma ray intensity and bulk density measurements of drill cores from the southern Georgina Basin with hyperspectral VNIR-SWIR-TIR drill core measurements showed a positive correlation between the total gamma ray intensity and the white mica and quartz abundance derived from hyperspectral data, as well as dolomite-dominated limestone corresponding to higher densities when compared to limestones with a mixed calcite-dolomite carbonate assemblage and elevated quartz abundance (Ayling et al., 2016).

Other petrophysical data, such as magnetic susceptibility and density, can be used when exploring for iron oxide copper-gold (IOCG) mineralisation by estimating proportions of magnetite, sulfide and hematite alteration (Hanneson, 2003). Magnetic susceptibility is mainly controlled by the abundance of magnetite or pyrrhotite, which also have a significant influence on the density of a rock sample (Ross et al., 2013). The impact of iron oxides and sulfides varies across the visible and infrared wavelength ranges. In single-mineral samples, each of them shows distinct absorption features in the VNIR. Hematite can be easily identified in VNIR reflectance spectra, even in a mixed mineral assemblage (Cudahy and Ramanaidou, 1997). Dependent on, for example, its relative abundance and grain size, magnetite can have a significant impact on SWIR reflectance spectral signatures of other minerals, obscuring the otherwise very strong hydroxyl-related absorptions of sheetsilicates. Furthermore, magnetite and pyrrhotite contribute to the "thermal background" in the TIR, which results in an increasing slope towards the 15,000 nm wavelength range (Feng et al., 2006).

Partial least squares (PLS)-based modelling of magnetic susceptibility and density was trialled using HyLogger3 data of drill core TTNQ0364 from the Osborne Cu-Au deposit (Qld, Australia) to investigate whether the combined use of hyperspectral reflectance spectra and petrophysical data could help with predicting and distinguishing between samples dominated by magnetite, hematite and or pyrrhotite from spectral data. Using TSG^{TM} software, PLS was employed to derive predictive models using 23 unique magnetic susceptibility and density measurements. Each of the 23 unique petrophysical measurements were set as a constant response variable for all spectral measurements over a +/- ~10cm sampling range. The values of the input magnetic sustainability and density values ranged from 0 to 2.3 K (Si) and 2.7 to 4.9 g/cm^3, respectively. Similar to the geochemical data of the Greenbushes case study described above, the measured petrophysical values likely represent an average over that range and the true petrophysical values might be very different for each of the 1 cm separated spectra. The correlation between the 23 measured and corresponding modelled magnetic susceptibility (n = 157) for the same 23 depth intervals was high for the VNIR-SWIR (r^2 = 0.95) and the TIR (r^2 = 0.97; Figure 2), but the standard error of prediction (SEP) was, compared to the actual value range, high (SEP for VNIR-SWIR: 0.35 Si; SEP for TIR: 0.32 Si). PLS-modelled magnetic susceptibility values showed a large variance (± 0.8 and ± 0.5 Si, respectively). Similarly, the correlation between the measured and modelled density was high for the VNIR-SWIR (r^2 = 0.958) and the TIR (r^2 = 0.99; Figure 2), with a high predictive error (SEP for VNIR-SWIR: 0.28 g/cm^3; SEP for TIR: 0.22 g/cm^3). The PLS-modelled density values showed a large variance (± 0.4 g/cm^3 for both wavelength ranges). However, HyLogger3 high-resolution RGB imagery showed that the predicted value ranges were sufficiently different to discriminate drill core intervals dominated by magnetite-rich rocks, from magnetite-rich breccia and least-altered (non-mineralised) rocks.

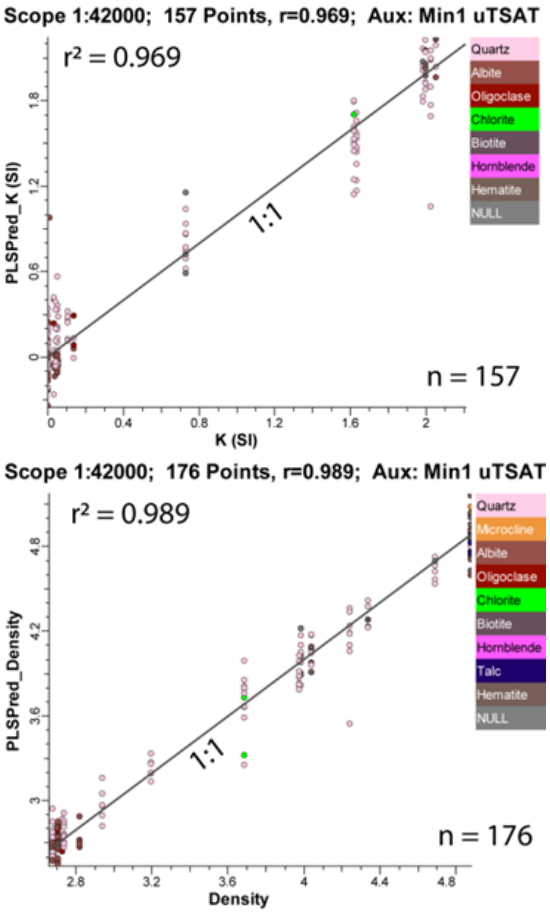

Figure 2. Measured (x-axis) versus PLS-modelling based petrophysical parameters (y-axis) of drill core TTNQ0364: (a) TIR-based PLS model of magnetic susceptibility K (Si); (b) TIR-based PLS model of density ρ in g/cm^3. Both plots are coloured by automated mineral matching results using the TSA-algorithm built into TSG^{TM}.

PLS models based on the VNIR-SWIR wavelength ranges were mainly driven by depth changes of electronic transition absorption features related to iron and copper in the VNIR, which are most intense in the highly altered, magnetite- and/or sulfide rich rocks. PLS models based on the TIR wavelength

ranges were highly influenced by the thermal background typically associated with iron oxides and sulphides, but also presence/absence of carbonates versus quartz, feldspar and/or sheetsilicates. The modelling was limited by potential non-linear relationships between magnetic susceptibility, density and the reflectance spectra and the small number of paired observations (23). This means that the developed PLS models are only just overdetermined and are unlikely to predict well. The model also assigned all nearby reflectance spectra to the unique magnetic susceptibility and density measurements and this may not be an appropriate way to relate these observations when using PLS models. This is because linear least-squares models like PLS can suffer from biases when there is a substantial error in the response variables, and this is the effective impact of using the same magnetic susceptibility and density measurements with multiple hyperspectral observations.

While the small amount of data used to infer the models discussed here means that their predictive power needs to be assessed comprehensively, our results nevertheless indicate a high potential for successfully inferring petrophysical from hyperspectral data and cost-effective mapping of IOCG-related alteration. The large range of predicted values for a given measurement can potentially be attributed to the significant variation of the respective petrophysical parameters within the original sampling range. It should also be noted that PLS-modelling uses a linear relationship between the input and the modelled data and it is unclear, at this stage, whether a linear relationship between the hyperspectral data on one side and the magnetic susceptibility or density on the other side can be assumed for the whole range of values present or even parts thereof.

CONCLUSIONS

A wide range of drill core analytical tools are available for objectively measuring geoscience parameters that aid mineral exploration or groundwater research (Laukamp et al., 2021a). The comparison and integration of hyperspectral with geochemical or petrophysical drill core data requires an understanding of mineral physicochemistry and rock properties that contribute to reflectance spectral signatures (e.g. grain size and porosity) so that correlations between hyperspectral, geochemical and petrophysical parameters can be explained in a causative sense.

Case studies from a wide range of geological environments that are based on NVCL drill core data sets available via AuScope's Discovery Portal highlight multiple challenges and opportunities with regards to extracting geoscience parameters from drill core data, such as 1) the requirement for understanding the limitations and potential of the respective drill core analytical technologies, 2) the underutilised potential for extracting geochemical exchange vectors from hyperspectral data, 3) lack of spatial co-registration of different drill core analytical measurements, 4) significant issues related to different sampling volumes and intervals of the respective drill core analytical techniques, and 5) the potential and limitations of PLS-modelling based prediction of geochemical and petrophysical data from hyperspectral data. Many of the issues described in the case studies are faced by geologists daily. AuScope's NVCL infrastructure program and database provides opportunities to explore the feasibility of extracting geoscience parameters from multiple types of drill core data and understanding their interrelations as well as the uncertainties in the observed relations.

ACKNOWLEDGMENTS

This work is part of the National Virtual Core Library (NVCL), which is funded by AuScope under the Australian Government's NCRIS scheme and CSIRO's Mineral Resources Business Unit.

REFERENCES

Ayling, B., Huntington, J., Smith, B., Edwards, D., 2016. Hyperspectral logging of middle Cambrian marine sediments with hydrocarbon prospectivity: a case study from the southern Georgina Basin, northern Australia. Aust. J. Earth Sci. 1–17.

Burns, R.G., 1993. Mineralogical Applications of Crystal Field Theory, 2nd ed. Cambridge University Press.

Clark, R.N., King, T.V.V., Klejwa, M., Swayze, G.A., Vergo, N., 1990. High spectral resolution reflectance spectroscopy of minerals. J. Geophys. Res. 95, 12653.

Cudahy, T.J., Ramanaidou, E.R., 1997. Measurement of the hematite:goethite ratio using field visible and near-infrared reflectance spectrometry in channel iron deposits, Western Australia. Aust. J. Earth Sci. 44, 411–420.

Dentith, M., Enkin, R.J., Morris, W., Adams, C., Bourne, B., 2020. Petrophysics and mineral exploration: a workflow for data analysis and a new interpretation framework. Geophys. Prospect. 68, 178–199.

Feng, J., Rivard, B., Gallie, E.A., Sanchez, A., 2006. Quantifying total sulfide content of cores and cut-rock surfaces using thermal infrared reflectance. Geophysics 71, M1–M9.

Hanneson, J.E., 2003. On the use of magnetics and gravity to discriminate between gabbro and iron-rich ore-forming systems. Explor. Geophys. 34, 110–113.

Laukamp, C., LeGras, M., Lau, I.C., 2021a. Hyperspectral proximal sensing instruments and their applications for exploration through cover, in: Crocombe, R. (Ed.), Portable Spectroscopy and Spectrometry 2: Applications.

Laukamp, C., LeGras, M., Montenegro, V., Windle, S., McFarlane, A.J., 2021b. Grandite-based resource characterisation of the skarn-hosted Cu-Zn-Mo deposit of Antamina, Peru. Mineralium Deposita 56.

Laukamp, C., Rodger, A., LeGras, M., et al., 2021c. Mineral Physicochemistry Underlying Feature-Based Extraction of Mineral Abundance and Composition from Shortwave, Mid and Thermal Infrared Reflectance Spectra. Minerals 11, 347.

McLeod, R.L., Gabell, A.R., Green, A.A., Gardavsky, V., 1987. Chlorite infrared spectral data as proximity indicators of volcanogenic massive sulphide mineralisation. Presented at the Pacific Rim Congress, Gold Coast, Queensland, Australia.

Ross, P.-S., Bourke, A., Fresia, B., 2013. A multi-sensor logger for rock cores: Methodology and preliminary results from the Matagami mining camp, Canada. Ore Geol. Rev. 53, 93–111.

Schodlok, M.C., Whitbourn, L., Huntington, J., et al., 2016. HyLogger-3, a visible to shortwave and thermal infrared reflectance spectrometer system for drill core logging. Aust. J. Earth Sci. 63, 929–940.

Vedder, W., McDonald, R.S., 1963. Vibrations of the OH Ions in Muscovite. J. Chem. Phys. 38, 1583–1590.

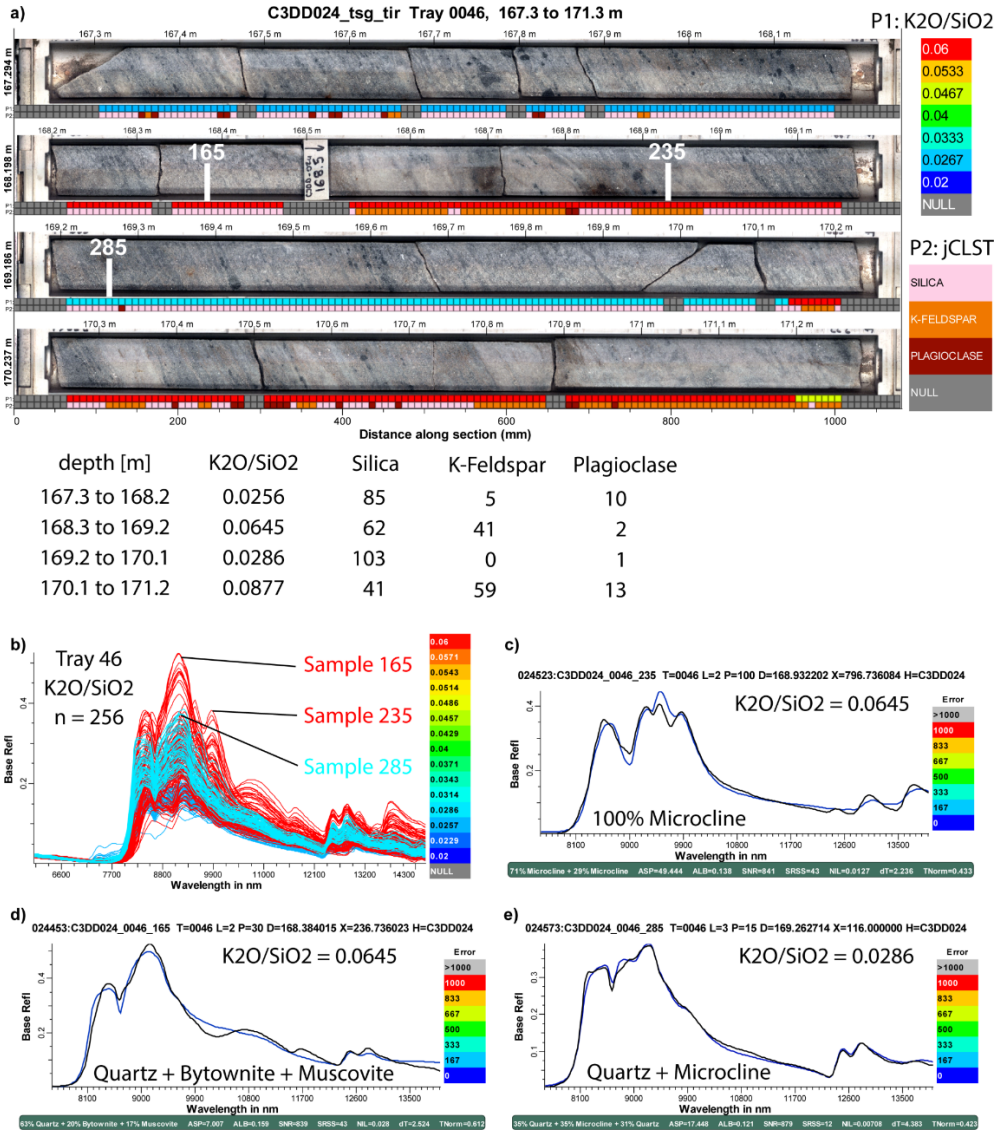

depth [m]	K2O/SiO2	Silica	K-Feldspar	Plagioclase
167.3 to 168.2	0.0256	85	5	10
168.3 to 169.2	0.0645	62	41	2
169.2 to 170.1	0.0286	103	0	1
170.1 to 171.2	0.0877	41	59	13

Figure 1. Comparison of major silicate mineral phases and K-content in tray 46 of drill core C3DD024 (Greenbushes, WA): a) Tray image of tray 46 with colour ribbons showing K_2O/SiO_2 (top ribbon, P1) and the number of pixels occupied by the most prominent mineral group according to jCLST (lower ribbon, P2). The table below the tray image lists the K_2O/SiO_2 values per 1 m whole rock geochemistry analysis and the number of pixels where silica, K-feldspar or plagioclase are classified by jCLST Grp1; b) TIR HyLogger reflectance spectra of tray 46, coloured by K_2O/SiO_2. Samples 165, 235 and 285 are highlighted in a) and b); c), d), e) TIR reflectance spectra of samples 165, 235 and 285, respectively (black lines) and jCLST modelling results (coloured line). Mineral modelling results based on jCLST are summarised for clarification in each of the diagrams.

Petrophysical method	**Petrophysical measurement**	**Correlated with mineral (wavelength region, in which respective minerals are active)**
Gamma logs	- K-channel - Th-channel - U-channel	- Mica (SWIR, MIR, TIR), K-feldspar (MIR, TIR) - Iron oxides (VNIR) - Selected sheet silicates, feldspars and phosphates
Density	mass of a substance per unit measure	"high" (i.e. > 5 g/cm^3): hematite, magnetite, pyrite (all VNIR) "medium" (i.e. 3 to 5 g/cm^3): dark mica (SWIR, MIR, TIR); garnet, olivine (TIR); sphalerite (VNIR) "low" (i.e. < 3 g/cm^3): calcite, kaolinite (SWIR, MIR, TIR); feldspar, quartz (MIR, TIR); halite (TIR)
Magnetic susceptibility	Dimensionless proportionality constant (expressed as volume, mass or molar susceptibility)	strong: magnetite (VNIR), pyrrhotite (VNIR) low: epidote (VNIR, SWIR, MIR, TIR)

Table 1. Petrophysical measurements commonly collected from drill cores and examples of mineral groups that contribute to respective petrophysical measurement and their IR-activity